Hydrol. Earth Syst. Sci., 14, 1449–1464, 2010
www.hydrol-earth-syst-sci.net/14/1449/2010/
doi:10.5194/hess-14-1449-2010

Hydrology and Earth System Sciences

The potential for remote sensing and hydrologic modelling to assess the spatio-temporal dynamics of ponds in the Ferlo Region (Senegal)

V. Soti[1,2,3], C. Puech[4], D. Lo Seen[3], A. Bertran[2], C. Vignolles[5], B. Mondet[6], N. Dessay[7,8], and A. Tran[2,3]

[1]SAS Nevantropic, 97300 Cayenne, French Guiana
[2]CIRAD, UPR AGIRs, 34398, Montpellier, France
[3]CIRAD, UMR TETIS, 34093, Montpellier, France
[4]CEMAGREF, UMR TETIS, 34093, Montpellier, France
[5]CNES, 31401, Toulouse, France
[6]IRD, UR 178, 34093, Montpellier, France
[7]IRD, UMR LTHE, 38400, Grenoble, France
[8]IRD, US ESPACE, 34093, Montpellier, France

Received: 16 December 2009 – Published in Hydrol. Earth Syst. Sci. Discuss.: 12 January 2010
Revised: 23 June 2010 – Accepted: 6 July 2010 – Published: 4 August 2010

Abstract. In the Ferlo Region in Senegal, livestock depend on temporary ponds for water but are exposed to the Rift Valley Fever (RVF), a disease transmitted to herds by mosquitoes which develop in these ponds. Mosquito abundance is related to the emptying and filling phases of the ponds, and in order to study the epidemiology of RVF, pond modelling is required. In the context of a data scarce region, a simple hydrologic model which makes use of remote sensing data was developed to simulate pond water dynamics from daily rainfall. Two sets of ponds were considered: those located in the main stream of the Ferlo Valley whose hydrological dynamics are essentially due to runoff, and the ponds located outside, which are smaller and whose filling mechanisms are mainly due to direct rainfall. Separate calibrations and validations were made for each set of ponds. Calibration was performed from daily field data (rainfall, water level) collected during the 2001 and 2002 rainy seasons and from three different sources of remote sensing data: 1) very high spatial resolution optical satellite images to access pond location and surface area at given dates, 2) Advanced Spaceborne Thermal Emission and Reflection Radiometer (ASTER) Digital Elevation Model (DEM) data to estimate pond catchment area and 3) Tropical Rainfall Measuring Mission (TRMM) data for rainfall estimates. The model was applied to all ponds of the study area, the results were validated and a sensitivity analysis was performed. Water height simulations using gauge rainfall as input were compared to water level measurements from four ponds and Nash coefficients >0.7 were obtained. Comparison with simulations using TRMM rainfall data gave mixed results, with poor water height simulations for the year 2001 and good estimations for the year 2002. A pond map derived from a Quickbird satellite image was used to assess model accuracy for simulating pond water areas for all the ponds of the study area. The validation showed that modelled water areas were mostly underestimated but significantly correlated, particularly for the larger ponds. The results of the sensitivity analysis showed that parameters relative to pond shape and catchment area estimation have less effects on model simulation than parameters relative to soil properties (rainfall threshold causing runoff in dry soils and the coefficient expressing soil moisture decrease with time) or the water loss coefficient. Overall, our results demonstrate the possibility of using a simple hydrologic model with remote sensing data to track pond water heights and water areas in a homogeneous arid area.

Correspondence to: V. Soti
(vs.nev@ntropic.fr)

Published by Copernicus Publications on behalf of the European Geosciences Union.

1 Introduction

Ponds and lakes are essential for life in the semi-arid Sahel region of Africa. Besides hosting a considerable biodiversity, these water bodies can be filled during the rainy season, and often remain the primary water supply for human and animal consumption. While being crucial for increasing aquifer recharge, these fragile aquatic ecosystems are subject to various natural (recurrent drought) or anthropogenic (overexploitation, dams, pollution, drainage) threats. Another major concern is that these water bodies are focal points where humans and livestock accede to water (Diop et al., 2004), and are at the same time favourable breeding sites for mosquitoes (Linthicum et al., 1985) that transmit various arboviruses, including those responsible for the Rift Valley Fever (RVF). RVF is an acute illness that affects humans and domestic ungulates (e.g. Wilson et al., 1994), and has an impact on the economy of the livestock sector. Water bodies in these regions therefore need to be closely monitored, not only as a resource in itself, but also in relation to the economy and public health of the region.

It is considered particularly challenging to characterize and survey water bodies located in these arid areas, because of the difficulty to obtain good quality data records of temporary and episodic floods in time and space (Lange et al., 1999). Numerous studies for monitoring water bodies have been conducted on large water areas using remote sensing, particularly in flood monitoring (Barton and Bathols, 1989; Sandholt et al., 2003; Montanari et al., 2009) or water storage in large lakes (Dingzhi et al., 2005). In arid areas, the potential of time series from coarse-scale satellites images like NOAA-AVHRR (Verdin, 1996), SPOT-Vegetation (Haas et al., 2006) or Terra-MODIS (Moderate Resolution Imaging Spectroradiometer) to survey large ponds and lakes at a broad spatial scale was demonstrated. Nevertheless, in the Sahel region, the spatial resolution of those sensors is inappropriate (Soti et al., 2009) for identifying water bodies with a surface area of less than 170 000 m^2 (Soti et al., 2009), which is the case for most of the ponds there. Recently, it was shown that the new generation of high and very high spatial resolution remote sensing data (Landsat Enhanced Thematic Mapper, SPOT5 and Quickbird images) is suitable for the detailed mapping of temporary water bodies at a local scale (Liebe et al., 2005; Lacaux et al., 2007; Soti et al., 2009). The potential of radar satellite images (Annor et al., 2009; Di Baldassarre et al., 2009; Schumann et al., 2009) for water body inventory have also been improved, with the advantage of being independent of cloud cover (Horritt et al., 2001; Herold et al., 2004). Thus, an efficient and simple method to study the spatial dynamics of temporary ponds would consist in mapping the ponds using satellite images acquired at different dates (Lacaux et al., 2007; Tourre et al., 2008). However, a daily follow-up is not possible with this approach, given the strong inverse relationship between spatial resolution and revisit time.

In order to access additional temporal information on pond dynamics, hydrologic models have been developed at the pond scale (Desconnets, 1994; Desconnets et al., 1997; Martin-Rosales and Leduc, 2003). Applications at a regional scale to monitor states of daily water bodies have been tested with success. These studies were generally based on volume-area-depth (V-h-A) mathematical relations (O'Connor, 1989; FAO, 1996; Hayashi and Van der Kamp, 2000; Liebe et al., 2005; Nilsson et al., 2008) and require a detailed bathymetry. The possibility of using remote sensing to improve water area estimation with these mathematical relations has also been investigated. Puech (1994) and Puech and Ousman (1998) showed that SPOT4 satellite images could be used with volume-area-depth relations to accurately estimate the volume of small water bodies of more than 10 ha, in the Tillabery region of North Niger. Recently, Liebe et al. (2005) and Annor et al. (2009) used similar relations but with radar images (ENVISAT ASAR) for water volume estimations of 21 small reservoirs ($<$30 ha) in East Ghana.

In this paper, we explore the possibility of developing a simple pond water balance model, requiring few input data and minimal parameterisation, that (i) takes advantage of available remote sensing data in an otherwise data scarce region, (ii) simulates water availability for herds, and (iii) renders pond water dynamics accurately enough to be subsequently used for studying the dynamics of mosquito abundance. The model developed uses three different sources of remote sensing data: 1) very high spatial resolution optical satellite images to access pond location and surface area at given dates, 2) ASTER (Advanced Spaceborne Thermal Emission and Reflection Radiometer) Digital Elevation Model (DEM) data to estimate pond catchment area and 3) TRMM (Tropical Rainfall Measuring Mission) data for rainfall estimates. After a brief presentation of the study area and available data sets (meteorological, hydrological, topographic, remote sensing images), a daily water balance model and a volume-area-depth model are described. Then, the paper presents the application of the model to the 98 ponds of the study area using daily field rainfall data (2001 and 2002) and TRMM data (2001, 2002, and 2007). Validations are carried on water height simulations with daily water height data collected for four ponds during the 2001 and 2002 rainy seasons, and also on water area simulations, using a pond map derived from a Quickbird image acquired on 20 August 2007. Results of a sensitivity analysis are also presented and discussed.

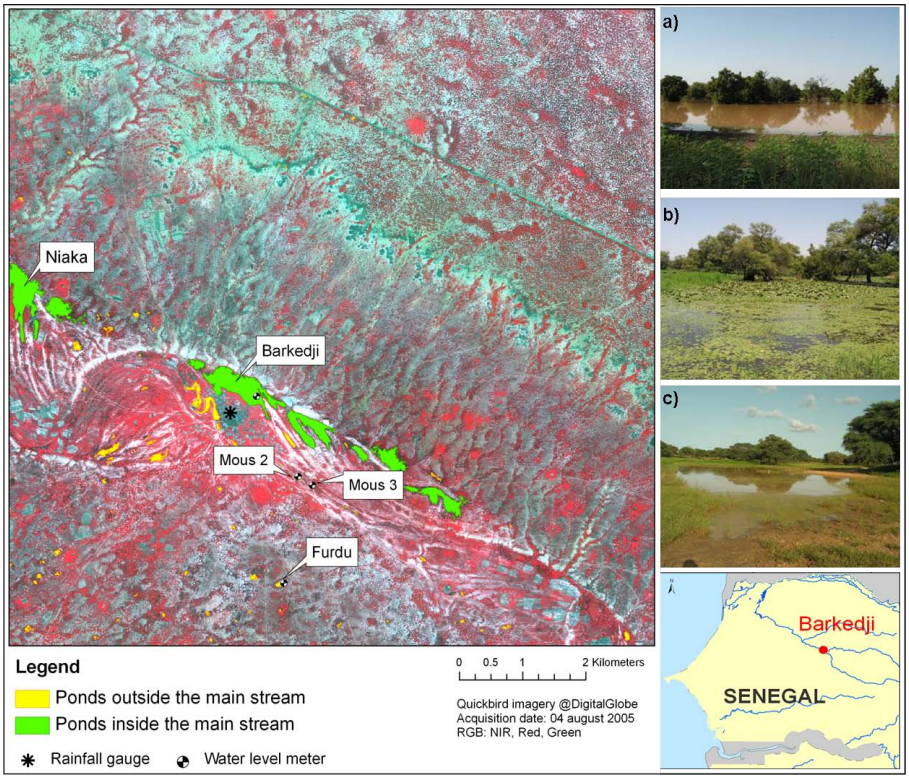

Fig. 1. Quickbird image of the study area showing location of ponds, rain gauge and water level meters near Barkedji village, Ferlo Region, Senegal. **(a)** Barkedji, **(b)** Furdu and **(c)** Mous3 ponds in September 2006.

2 Material and methods

2.1 Study area

The study area (Fig. 1) is located in the Ferlo Valley, North Senegal, and covers an area of 11 km×10 km around the village of Barkedji (15.28° N–14.87° W). The relief is characterized by low altitude (25 m average) and composed of a lateritic crust partially covered by flattened dunes and stabilised by vegetation (Le Houerou, 1988; Pin-Diop et al., 2007). This plateau was eroded by a former affluent of the Senegal River, the Ferlo River. The study area is located between isohyets 300 mm and 500 mm and has a Sahelian climate characterized by two seasons: a dry season which is dry and cold from November to March, and dry and hot from April to June, and a rainy season from June to November (Ndiaye, 2006). D'Amato and Lebel (1998) estimated that mean rainfall intensity in the Sahel is about 15 mm/day during the rainy season. Nevertheless, in this region, rainfall events have a convective origin (Lebel et al., 2003) and thus are highly variable in space and time (D'Amato and Lebel, 1998; Vischel and Lebel, 2007; Wheater et al., 2007). The temporal rainfall distribution is extremely irregular and is characterized by local dry spells lasting generally more than 5 days (Frappart et al., 2009). For example, Balme at al. (2006) estimated from 13 year time series of a 30 stations rain gauge network distributed within an area of $110\times160\,km^2$ in the region of Niamey, that 20% of the total annual rain falls with intensities $>78\,mm\,h^{-1}$, and 50% with intensities $>35\,mm\,h^{-1}$. In Barkedji area, annual temperature varies between 21.2 °C and 36.6 °C with an average of 29.6 °C and an average annual evaporation of 4.6 mm/day (Diop et al., 2004). The annual rainfall was 415 mm in 2001 and 296 mm in 2002, with a marked deficit of 30% for the latter.

The study area is characterized by an ensemble of ponds that are filled during the rainy season (from July to mid-October). Generally, the limits of these ponds are delineated by a belt of trees which corresponds to the maximum water extension. Most of the ponds in the study area are small (33% of ponds with an area less than $1000\,m^2$ and 64% with less than $2600\,m^2$), with the smallest one covering only $74\,m^2$ and the largest one, Barkedji, covering $\sim347\,400\,m^2$ (Soti et al., 2009). The larger ponds are located in the main stream of the Ferlo valley and the smaller ones generally outside. During the rainy season, the temporary ponds are quickly filled in successive occasions in the very few hours during and after the shower, whereas the emptying phase lasts longer, between a few days and several months after the last precipitation event (Martin-Rosales and Leduc, 2003). All ponds dry out during the dry season.

Field data that were used to build, calibrate and validate the model were collected on five ponds of the study area. The two larger ponds (Barkedji and Niaka) belong to the main stream, whereas the three smaller ones (Furdu, Mous 2 and Mous 3) are found outside the main stream. The locations of the five ponds are shown in Fig. 1, together with pictures of Barkedji, Furdu and Mous 3 ponds taken during the 2006 rainy season.

2.2 Meteorological data

Two sets of rainfall data were used:

- Daily rainfall data collected from July to December (rainy seasons of 2001 and 2002) using an automatic meteorological collector (WM 918 from Skyview Systems Ltd) and a meteorological station (Weather View Ltd) located in the village of Barkedji.
- Daily TRMM rainfall data (3B42-V6 product) with a $0.25^\circ \times 0.25^\circ$ spatial resolution. TRMM data corresponding to the study area have been downloaded from the NASA's Goddard Earth Sciences Data and Information Services Center for the rainy seasons of 2001, 2002 and 2007 (http://disc2.nascom.nasa.gov/Giovanni/tovas/TRMM_V6.3B42_daily.2.shtml).

2.3 Hydrological data

Water height data were collected daily from July to December in 2001 and 2002 from water level meters placed at the deepest point of four ponds, namely Barkedji, Furdu, Mous 2 and Mous 3 (Fig. 1). For the study, we used the Mous 2, Mous 3 and Furdu water height data collected during the two years – 2001 and 2002. For Barkedji, the water level readings for the first season (2001) were unexploitable due to a technical problem (displacement of the meter) that was not detected and corrected early enough. Therefore, only water height data collected during the 2002 rainy season were used for this pond.

2.4 Topographic data

2.4.1 Pond shape data used for the volume-area-depth model

Elevation data was obtained in May 2003 using an electronic Theodolite (T.I 1600 series) during a detailed survey of Niaka pond located in the main stream of the Ferlo valley and Furdu pond located outside (Fig. 1). Points were surveyed with a 2 to 5 m horizontal spacing and then interpolated on a regular 2 m grid.

2.4.2 ASTER Digital Elevation Model (DEM) used for catchment delineation

A DEM with 30 m pixel size covering the whole study area was downloaded from the ASTER Global DEM dataset of the NASA's Warehouse Inventory Search Tool (WIST) website (https://wist.echo.nasa.gov/wist-bin/api/ims.cgi?mode=MAINSRCH\&JS=1). The ASTER DEM was used to estimate the catchment area of the bigger ponds, located inside the main stream.

2.5 Pond maps

Two pond maps of the study area were extracted from Quickbird satellite images acquired in 2005 and 2007 (see Table 1). The procedure included thresholding the Normalized Difference Water index (NDWI, McFeeters, 1996) which is known to be suited for water bodies extraction (Soti et al., 2009). The 2005 image was acquired at the peak of a higher than normal rainfall season, when ponds were expected to be at their maximum. It was used for extracting pond parameters, and more specifically the maximum surface area for each pond, in order to estimate catchment areas of the ponds located outside of the main stream. The 2007 image was used to validate the water areas predicted by the model. The 2005 pond delineation had been systematically verified during a field survey (using a Global Positioning System receiver) in September 2006 at the peak of the rainy season (Soti et al., 2007). The data used in the study are summarized in Table 1.

3 Modelling overview and methods

We developed a simple hydrological model that simulates the main pond filling and emptying processes. For the study, we considered two sets of ponds: those located in the main stream of the Ferlo Valley (set 1) whose hydrological dynamics are due essentially to runoff, and the ponds located outside (set 2), which are smaller and whose filling mechanisms are mainly due to direct rainfall (Fig. 1). Then, separate calibrations and validations were performed for each set. The first two parts of this section will be dedicated to the hydrological model description (§3.1 and §3.2). The following parts explain the model parameters estimated from field data (§3.3) and remote sensing data (§3.4). Then, model calibration, model validation and the sensitivity analysis are described in §3.5, §3.6 and §3.7 respectively.

3.1 Hydrologic model description

A daily water balance model is used to predict volume, surface and height of temporary ponds of Barkedji study area (Fig. 2a). The relation between water volume, surface and height of a given pond depends on the 3-D shape of that pond. It is modelled here by two simple volume-depth (V-h) and area-depth (A-h) empirical equations that are described

Table 1. Summarized characteristics of the data used.

Data	Acquisition date	Complementary information	Sources
Rainfall data from a meteorological station	– From 01/07/2001 to 31/10/2001 – From 15/06/2002 to 31/10/2002	Daily data collected from a station located in the Barkedji village centre	IRD (France), CIRAD (France), ISRA (Senegal)
Rainfall data from TRMM satellite (3B42-V6)	– From 01/07/2001 to 31/12/2001 – From 15/06/2002 to 31/10/2002 – From 01/06/2007 to 31/12/2007	Daily, 27×27 km pixel size Joint US-Japan satellite mission to monitor tropical and subtropical precipitation	NASA Goddard Earth Sciences Data and Information Services Center
Water height data	– From 01/07/2001 to 31/12/2001 – From 15/06/2002 to 31/10/2002	– Furdu, Mous2 and Mous3 ponds – Barkedji, Furdu, Mous2 and Mous3 ponds	IRD (France), CIRAD (France), ISRA (Senegal)
Pond map	04/08/2005 20/08/2007	Derived from Quickbird images 2.47 m pixel size, Bands: B, G, R, NIR * 2005: used for the extraction of the maximum surface of each pond – A_{max} 2007: used for validation of pond areas	CIRAD (France), IRD (France), ISRA (Senegal).
DEM (ASTER)	2009	30 m pixel size	METI (Japan), NASA (USA)
Detailed DEM	May 2003	Furdu and Niaka ponds (2 m pixel size)	IRD (France)

* B: Blue; G: Green; R: Red; NIR: Near Infrared.

in more detail in the next paragraph. The general volumetric water balance of a pond is given by:

$$\frac{dV}{dt} = P(t)\,A(t) + [Q_{in}(t) - Q_{out}(t)] - L\,A(t) \quad (1)$$

The first term is the contribution from direct rainfall, expressed as the product of rainfall $P(t)$ and water body surface area $A(t)$. Q_{in} is the runoff volume of inflows, Q_{out} the runoff volume of outflows and L the water loss per unit surface area through evaporation and infiltration. The model was implemented with a daily time step. For the study, each pond was considered a closed water body, and it was assumed no hydrological connexion between ponds ($Q_{out} = 0$). Thus we did not model extensive flood events which are very unusual in the study area. The formulation proposed by Girard (1975) was used for $Q_{in}(t)$ estimation, as it is considered particularly suited for studying small catchments of less than 100–150 km^2 located in the Sahel region (Dubreuil, 1986). $Q_{in}(t)$ is written as the product of a runoff coefficient (K_r), the effective rainfall (P_e) and the catchment area (A_c):

$$Q_{in}(t) = K_r\,P_e(t)\,A_c \quad (2)$$

The soil capacity to runoff was supposed uniform over the study area, and defined by a constant K_r coefficient. This constant takes implicitly into account the losses due to evapotranspiration and infiltration in the catchment area.

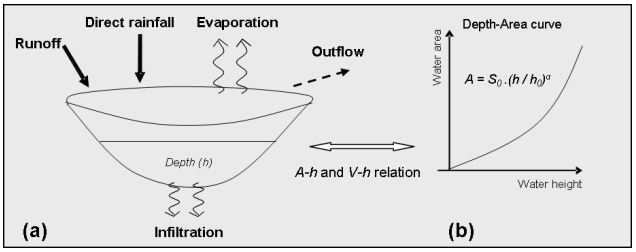

Fig. 2. Schematic representation of the hydrologic model. **(a)** Water balance model. **(b)** Area-depth relation.

The effective rainfall (P_e) corresponds to the part of the precipitation that produces runoff. P_e is calculated as follows:

$$P_e(t) = \max[P(t) - G(t), 0] \tag{3}$$

In Eq. (3), $G(t)$ is a variable which can be interpreted as a threshold rainfall value over which runoff can occur. $G(t)$ is defined by the difference between its maximum value $G_{\max}$ corresponding to a dry soil, and an Antecedent Precipitation Index (I_{ap}):

$$G(t) = \max[G_{\max} - I_{\text{ap}}(t), 0] \tag{4}$$

The I_{ap} Index (Kohler and Linsley, 1951) is a weighted summation of past daily precipitation amounts, used as an indicator of the amount of water in the soil and calculated as follows:

$$I_{\text{ap}}(t) = \left[I_{\text{ap}}(t-1) + P(t-1)\right] k \tag{5}$$

where $I_{\text{ap}}\ (t-1)$ is the I_{ap} index at the time step $(t-1)$, k is a dimensionless coefficient between 0 and 1 expressing the soil moisture decrease with time, and $P(t-1)$ is the rainfall at time step $(t-1)$. Because of the high spatial variation of the precipitation events in the Sahel, the $I_{\text{ap}}(t)$ index is also spatially variable within this region and, as such, cannot be compared between sites (Anctil et al., 2004).

Except during important rainfall events, water losses in such areas are known to be mainly due to evaporation (Puech, 1994). During rainfall events, infiltration could be important only when water level rises above the clogged area located at the bottom part of the pond (Diop et al., 2004; Porphyre et al., 2005). In this study, we followed Joannes (1986) and Puech (Puech, 1994) in assuming that water losses can be simply summarized through a constant L. All parameters and variables of the model are summarized in Table 2.

3.2 The volume-area-depth model

We used two simple volume-depth (V-h) and area-depth (A-h) equations to assess the volume-area-depth relations of the ponds of the study area (Fig. 2b). Such mathematical relations have been used with efficiency during modelling studies on temporary ponds (Puech, 1994; Hayashi and Van der Kamp, 2000; Nilsson et al., 2008; Annor et al., 2009) and lakes (Gates and Diessendorf, 1977; O'Connor, 1989; Bengtsson and Malm, 1997).

The empirical relation between pond area A and water depth h, and that between pond volume V and water depth h, are given in Eqs. (6) and (7) respectively:

$$A(t) = S_0 \left(\frac{h(t)}{h_0}\right)^{\alpha} \tag{6}$$

$$V(t) = V_0 \left(\frac{h(t)}{h_0}\right)^{\alpha+1} \text{ with } V_0 = \frac{S_0\, h_0}{\alpha+1} \tag{7}$$

where $A(t)$ is the pond area at time t,
$h(t)$ is the pond water height at time t,
S_0 is the water area for h_0= 1 m water height in the pond (Table 2),
α is a shape parameter representative of the slope profile (Table 2),
$V(t)$ is the volume of the pond at time t,
V_0 is the volume for h_0=1 m water height in the pond.

3.3 Estimation of pond shape parameters

The parameters α andS_0 were estimated for each of the two sets of ponds using the detailed bathymetry from Niaka and Furdu ponds, assuming that they are representative of the ponds of set 1 and set 2 respectively. Using a Geographic Information System (GIS) water area and water volume were calculated for several depths from the detailed DEM (Nilsson et al., 2008) of the two ponds. S_0 and α parameters were then estimated by fitting Eqs. (6) and (7) with the DEM derived water area and water volume. As error function to be minimized, we used the root-mean-squared error (RMSE) A_{err} defined as:

$$A_{\text{err}} = \sqrt{\frac{1}{m}\sum_{i=1}^{m}(A_{\text{obs}}(i) - A_{\text{sim}}(i))^2} \tag{8}$$

where A_{obs} is the area calculated from DEM, and A_{sim} is the area given by the power function, and m is the number of data points.

3.4 Estimation of catchment areas

For each pond of the main stream (set 1) characterized by an important runoff, we calculated the catchment area from the ASTER DEM using a GIS.

Outside the main stream, where ponds are generally smaller (set 2), slopes were too flat to be detected in the available DEM. For these ponds the catchment areas were empirically estimated as n times the maximum water surface area ($A_{\max}$) of the ponds (Table 2) as follows:

$$A_c = n\, A_{\max} \tag{9}$$

Table 2. Parameters and variables of the hydrologic pond model.

	Parameters and variables	Value/Range of values/ equation	Unit	Reference
Input variables				
P	Rainfall	$0 < P < 0.045$	m day^{-1}	Field survey
State variables				
V	Pond volume	Eq. (1)	m^3	
A	Pond surface area	Eq. (6)	m^2	
h	Pond water height	Eq. (7)	m	
Parameters				
A_c	Catchment area	0–150	km^2	(Dubreuil, 1986)
K_r	Runoff coefficient	0.15–0.40	dl*	(Girard, 1975)
α	Water body shape factor	1–3	dl	(FAO, 1996; Puech and Ousmane, 1998)
S_0	Water body scale factor	Depending on the water bodies	m^2	(D'At de Saint Foulc et al., 1986)
$G_{\max}$	Rainfall threshold value to start runoff in dry soils	10–20	mm day^{-1}	(FAO, 1996)
L	Water losses per day	5–20	mm day^{-1}	(Piaton and Puech, 1992)
k	Dimensionless coefficient expressing the soil moisture decrease in time	0–1	dl	(Heggen, 2001)
n	Number of times the catchment area of a small pond is larger than the maximum pond surface area	1–20	dl	See calibration

*dl: dimensionless

3.5 Model calibration

For set 1, the model was calibrated using 2002 gauge rainfall and water height field data of 2002 from Barkedji pond. For set 2, the model was calibrated using 2001 gauge rainfall and water height field data from Furdu. The model was computationally not expensive and it was possible to perform a systematic exploration of the input parameter space (Table 3). All possible combinations of parameter values in a range of values based on published literature (Table 2) but pertaining to similar sahelian regions, were considered.

For the calibration criteria, we used the coefficient of efficiency (Nash and Sutcliffe, 1970) which is expressed as follows:

$$C_{\text{eff}} = 1 - \frac{\sum_{i=1}^{m} (\text{Xobs}(i) - \text{Xcal}(i))^2}{\sum_{i=1}^{m} \left(\text{Xobs}(i) - \overline{\text{Xobs}}(i)\right)^2} \quad (10)$$

with m = number of observed data

where Xobs is the observed water height data; Xcal is calculated with the model and $\overline{\text{Xobs}}$ is the average of the observed water height data. Nash-Sutcliffe efficiencies can range from -∞ to 1. The closer the coefficient of efficiency is to 1, the more accurate the model is.

Table 3. Calibration experimentation plan.

	Total number of runs: 832 000			
Parameters	Min	Max	Step	Nb
K_r	0.17	0.30	0.01	26
$G_{\max}$ (mm day^{-1})	13	16	1	10
k	0.1	0.6	0.1	10
L (mm day^{-1})	10	16	1	16
n	1	20	1	20

3.6 Model validation

The model was run for 2001 and 2002 rainy seasons both from rain gauge and TRMM rainfall data. For the year 2007,

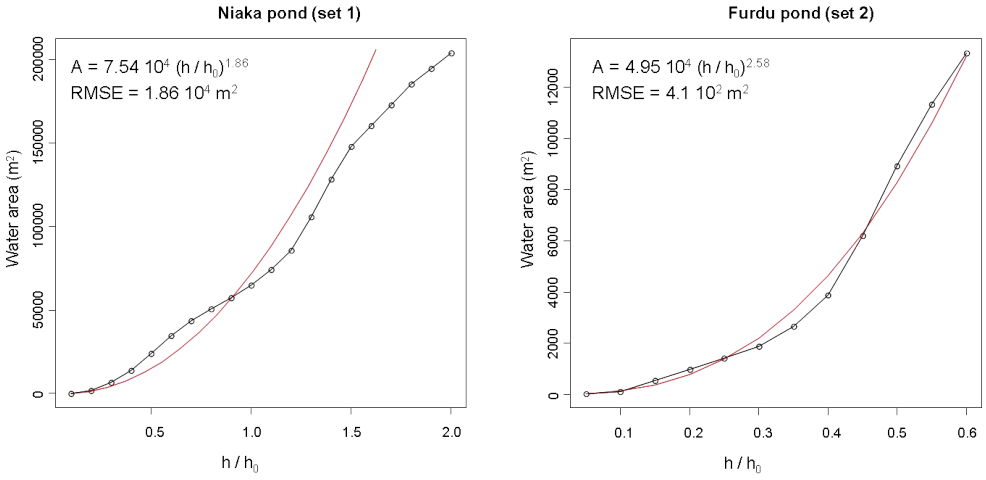

Fig. 3. Water area and water height relations for Niaka and Furdu ponds, Barkedji area, Ferlo region, Senegal.

rain gauge data were unavailable, and model simulation was run only with TRMM rainfall data, from 1 June 2007 to 31 December 2007.

The validations were carried out in two steps. First, on water height, internal validation was performed on Barkedji pond, and external validations on Furdu, Mous 2 and Mous 3 ponds, with 2001 and 2002 water level and rain gauge daily measurements. Then, simulated water areas were compared to water areas obtained from the 20 August 2007 Quickbird image. To evaluate the quality of the simulations, Nash coefficients (Eq. 10) were computed from simulated and observed water height temporal profiles, and a RMSE (Eq. 8) was calculated between simulated and observed water areas of the 98 ponds, on the date the Quickbird image was acquired.

3.7 The sensitivity analysis

A sensitivity analysis (SA) was carried out to assess the sensitivity of the model to the main model parameters, namely, the size of the catchment area A_c (and indirectly n for ponds of set 2), the pond shape parameters (S_0 and α) and the other parameters obtained by calibration (K_r, $G_{\max}$, k, L). The method used is the OAT (one-factor-at-a-time) Morris method (Morris, 1991), as revised by Campolongo (1999). The new method, in addition to the "overall" sensitivity measures already provided by the traditional Morris method, offers estimates of the two-factor interaction (Campolongo and Braddock, 1999; Saltelli et al., 2004). The parameters and their ranges used in the analysis are shown in Table 3. The variation space of the pond shape parameters S_0 and α was defined by their value estimated from field data (see §3.3) $\pm$10% and a uniform distribution.

Sensitivity estimates of the total effects due to a single parameter are produced by sampling the whole parameter space and obtaining a distribution of the elementary effects of a given parameter on the simulations. A mean (μ^*, calculated on absolute values) and variance (σ) can then be calculated from that distribution. A high mean indicates a parameter with an important effect on the output, whereas a large variance indicates either a factor interacting with another factor, or a factor whose effect is non-linear. Three outputs have been tested: (1) the cumulated water height, (2) the maximum water height and (3) the occurrence of the first peak in water height.

4 Results

4.1 S_0 and α estimations for V-A-h relation

The power functions that approximate the A-h relations of the Furdu and Niaka ponds are shown in Fig. 3. The two ponds are small and that is reflected in the range of the scaling constant S_0. The parameter α has low values, 1.86 for Niaka and 2.58 for Furdu pond which indicate that the depressions have a reasonably smooth and near-parabolic shape. In Niaka slopes are weaker than in Furdu. Errors between the observed data and values calculated by the power function are much more important for Niaka pond especially for water levels above 1.5 m.

4.2 Catchment areas (A_c)

The catchment areas of the largest ponds of the study area (set 1) were delineated using the ASTER DEM (Fig. 4). In total, 6 catchments have been extracted, with sizes ranging from 30 to 1107 ha. All catchments are located on the northern side of the valley where slopes are higher, around 5–8%. In the southern part, slopes are around 0–1% and the small ponds are numerous.

For the ponds located outside of the Ferlo main stream (set 2), the catchment areas were empirically estimated as n

Table 4. Model parameters values resulting from the calibration phase.

Parameters	Barkedji (set 1)	Furdu (set 2)
K_r	0.21	0.19
$G_{\max}$(mm day^{-1})	15	15
k	0.4	0.5
L (mm day^{-1})	15	12
n	–	10
Nash coef.	0.82	0.87

times the maximum water surface area of the ponds. A value of n=10 was obtained during the calibration phase (Table 4). Thus, the mean catchment size was 42 m^2 with a maximum of 381 m^2.

4.3 Model calibration results

The K_r, $G_{\max}$, k and L parameter values were estimated from model calibration for the two sets of ponds. High Nash-Sutcliffe values were obtained (Table 4). The result of the calibration gave an optimal Nash-Sutcliffe coefficient of 0.82 (set 1) for Barkedji pond in 2002 and 0.87 (set 2) for Furdu pond in 2001. It could be observed that parameter values obtained for the two sets are very similar.

Figure 5 compares model simulations of the different filling and emptying phases with water level records. It could be observed that the model simulates well the first rain events for Furdu, whereas the first peak rainfall is overestimated for Barkedji pond. Moreover, the water losses seem to be underestimated for the emptying phase for Barkedji.

4.4 Model validation results

4.4.1 Pond water height estimations

Because of the lack of water level records for Barkedji in 2001, only an internal validation was possible. For set 2 ponds, validation of model simulations using rain gauge inputs showed high Nash-Sutcliffe coefficients for both rainy seasons 2001 and 2002, with higher values in 2001. These values are given in Table 5, which summarizes the validation of model simulations using either rain gauge or TRMM as input. Higher Nash-Sutcliffe coefficients were obtained for the larger Furdu and Mous 3 ponds with respectively 0.83 and 0.73 in 2002. A lower correlation was observed for Mous 2, the smaller pond, with 0.67 in 2001 and 0.66 in 2002.

With TRMM rainfall estimates as model input, water height was not well simulated for all ponds during year 2001 and particularly for the smaller Mous 2 and Mous 3 ponds. However, for the rainy season 2002, results were acceptable with Nash-Sutcliffe coefficients of 0.73, 0.66 and 0.55 for Furdu, Barkedji and Mous 3 ponds respectively. Again, the correlation was not significant for the smallest pond, Mous 2 with a Nash-Sutcliffe coefficient of 0.42. Rain gauge measurements and TRMM estimates of 2002 are compared in Fig. 6, which also shows water height simulations obtained for Furdu and Barkedji. Rainfall statistics of rain gauge data and TRMM estimates are compared and shown in Table 6 and Fig. 6. TRMM is found to underestimate maximum and total rainfall, whereas rain gauge may miss rain events that are captured by TRMM.

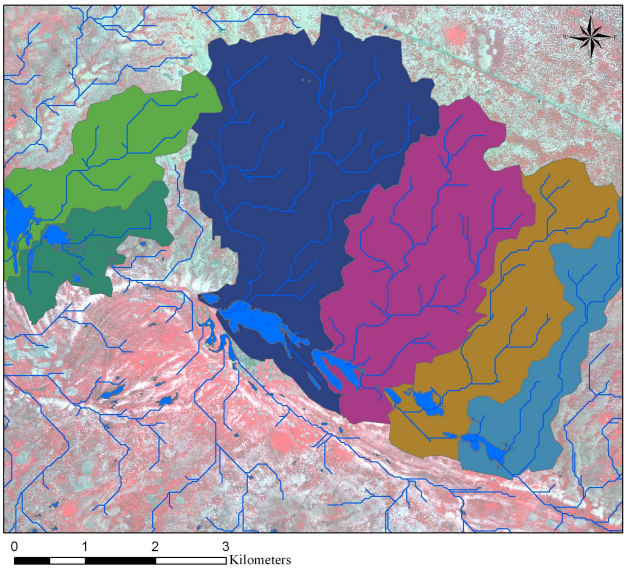

Fig. 4. Catchment area delineation using ASTER DEM. Ferlo valley, Senegal.

4.4.2 Pond water area estimations

Pond areas simulated for 20 August 2007 were compared with pond surface areas obtained from the QuickBird image of the same date. That image did not cover the whole study area, and only 71 ponds were concerned. The result (Fig. 7a) shows significant correlations with a coefficient of determination (r^2) of 0.89. A better fit was observed for the larger ponds of the study area. In Fig. 7b, surface area underestimation for some ponds could be observed.

4.5 Sensitivity analysis results

From the graphs shown in Fig. 8, different groups of parameters can be distinguished: a first group of parameters with low μ^* and σ values indicating a low effect on the outputs and a linear relation without interaction; a second group with intermediate μ^* values around 0.5 and with low σ values indicating a linear relation without interaction; and a last group with high μ^* and σ values in which the parameters have a significant effect on outputs and show some interactions or non-linear effects. Overall, it can be observed that all parameters

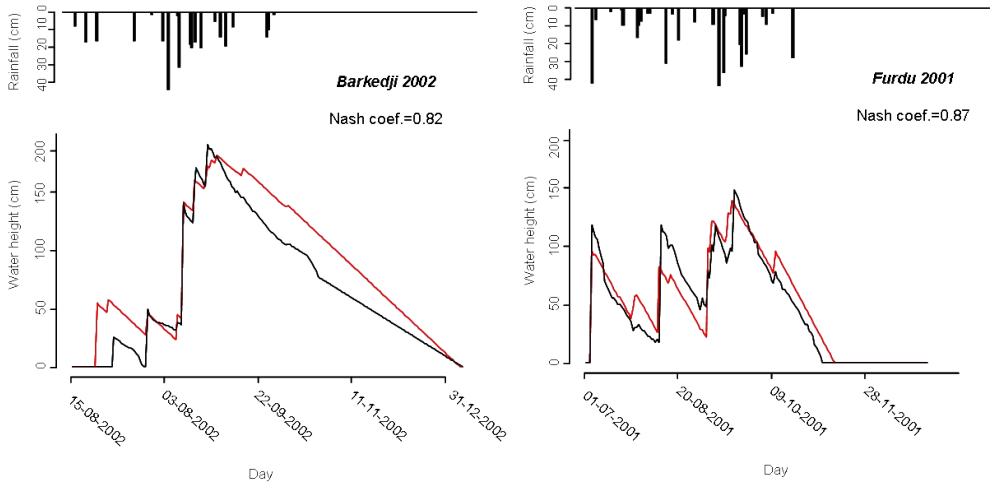

Fig. 5. Comparison of pond water height simulation (in red) using input parameters obtained from calibration, with water level records (in black) for Barkedji pond in 2002 (left) and Furdu pond in 2001 (right).

have an influence on outputs, meaning that the model reacts consistently with the hydrological processes modelled and that it could not be simplified with the elimination of more parameters. For the three outputs considered, A_c, K_r and S_0 are the parameters having the least effects, whereas those having more significant effects are k, $G_{\max}$ and L.

On the output sum of simulated water height (Fig. 8a), three groups of parameters can be identified: those with less effects (A_c, S_0 and K_r), or with moderate effects ($G_{\max}$, L, α), and k having the most effect on the output, with no interaction with other parameters. For the maximum of simulated water height output (Fig. 8b), parameter groupings are almost the same, except for $G_{\max}$ being the parameter with the most effect on the output and no interaction with other parameters. For the third output (Fig. 8c) which is the date of the first peak in water height, the influence of the parameters are negligible or low, except for k and the $G_{\max}$. These two parameters related to runoff have an important effect on the output, with high values of μ^* and σ. These suggest that the two parameters may be correlated or have a non-linear effect on the output. Conversely, parameters related to the pond shape have no influence.

5 Discussion

In this paper, a simple hydrological model was used to simulate daily water level variations. With the use of remote sensing data (Quickbird imagery, ASTER DEM, and rainfall data from TRMM satellite), the application of the model to the ponds (98) of the study area gave fair results both for water height and water area predictions.

5.1 Model calibration

The runoff coefficient (K_r), the rainfall threshold value to start runoff in dry soils ($G_{\max}$), the coefficient expressing the soil moisture decrease in time (k) and the water losses per day (L) were separately estimated from model calibration for the two sets of ponds: those inside (1) and outside (2) the main stream of the Ferlo River. The values of k is lower (0.4 and 0.5 for set 1 and set 2, respectively) than the usual values ranging between 0.80 and 0.98 (Heggen, 2001) This result is consistent with the work of Girard (1975), who showed that this parameter takes lower values in the Sahelian region because of a high evapotranspiration potential (around 250 mm per month). Moreover, the values obtained were very similar between the two sets of ponds. The main difference was obtained for L, which is lower for set 2. An explanation could be that because the ponds located outside the main stream are smaller, when water decreases, the clogged area located at the bottom part of the pond, where infiltration is less important (Diop et al., 2004; Porphyre et al., 2005), is reached more rapidly.

5.2 Estimation of pond shape parameters

The shape of any pond of our study area was summarized by the two parameters of a power law, S_0 and α. These parameters were estimated from the detailed DEM of two ponds, Niaka and Furdu, which were assumed to be representative of set 1 and set 2, respectively. This assumption could not be verified with appropriate DEM data. However, validation results carried out with water level records on several ponds, combined with a sensitivity analysis that reveals a low to moderate effect of S_0 and α on model outputs, suggest that the assumption was acceptable. In this way, the model could be applied to all the remaining ponds for which

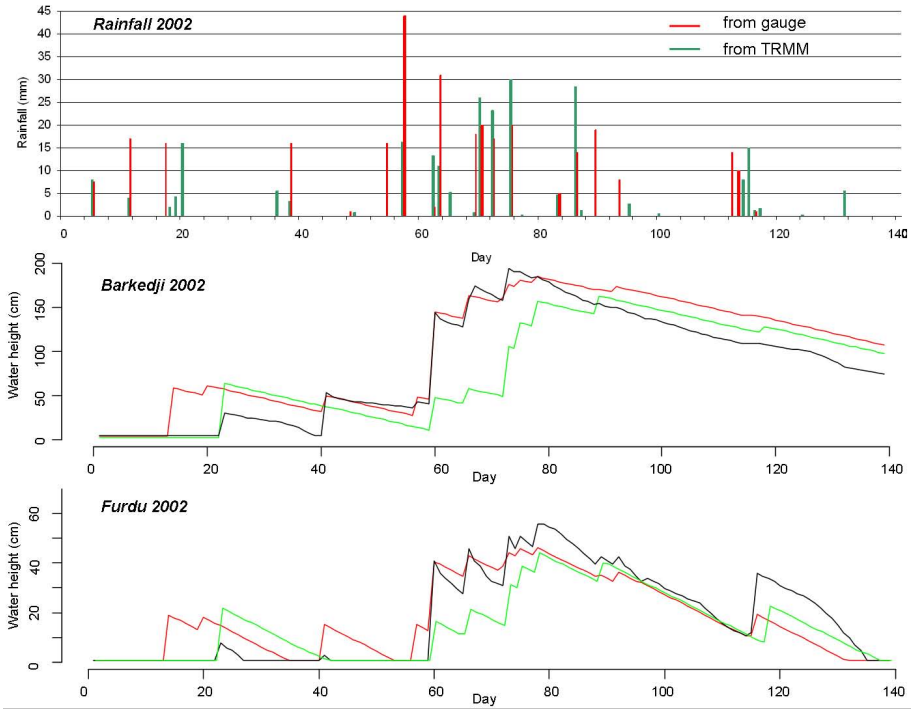

Fig. 6. Comparison of water heights field data (in black) with water heights simulated data from gauge rainfall (in red) and TRMM rainfall data (in green). Day 1 = 15 June 2002.

Table 5. Nash coefficients for comparing water height simulations and measurements (in italic: values obtained when measurements were also used for calibration).

Pond name	Max area (m^2)	Rainfall data from gauge			Rainfall data from TRMM		
		2001–2002	2001	2002	2001–2002	2001	2002
Barkedji	336 211	–	–	*0.82*			0.66
Furdu	10 005	0.87	*0.87*	0.83	0.61	0.39	0.73
Mous 2	500	0.70	0.67	0.66	0.30	0.06	0.42
Mous 3	3340	0.83	0.84	0.73	0.40	0.06	0.55

a detailed DEM/bathymetry were not available. The differences between the observed data and values calculated by the power function are low for Furdu pond (set 2). They are more important for Niaka pond, where the error induced in the estimation of the surface from the height estimation may reach 5 ha for Niaka pond for water heights of about 2 m. However, for this pond, maximum water height is about 1.2 m (height observed in 2003 which was a particularly wet year), implying that at 2 m water height, we are probably outside Niaka pond.

5.3 Sensitivity analysis

The sensitivity analysis (SA) was very useful to point up which factors are to be more accurately estimated on the field. Overall, the SA showed that G_{max}, k and L are the parameters with the most effects on model outputs, and which have to be well estimated. Conversely, topographic parameters (catchment area estimation and pond shape parameters) have less influence, suggesting that the errors in estimating catchment area from ASTER DEM, or from pond maximum surface area, may not be too penalising. Moreover, as stated above, this justified the application of the shape parameters (S_0 and α) to all ponds of the study area, although they were estimated from field data only for two ponds assumed representative.

Table 6. Comparison between rain gauge and TRMM estimates for 2001 and 2002.

	Daily max (mm)	Total (mm)	Number of rainy days (>1 mm)	Nash	R
TRMM 2001	44	360	27	0.03	0.58
Gauge 2001	45	416	27		
TRMM 2002	30	239	23	0.28	0.46
Gauge 2002	44	297	20		

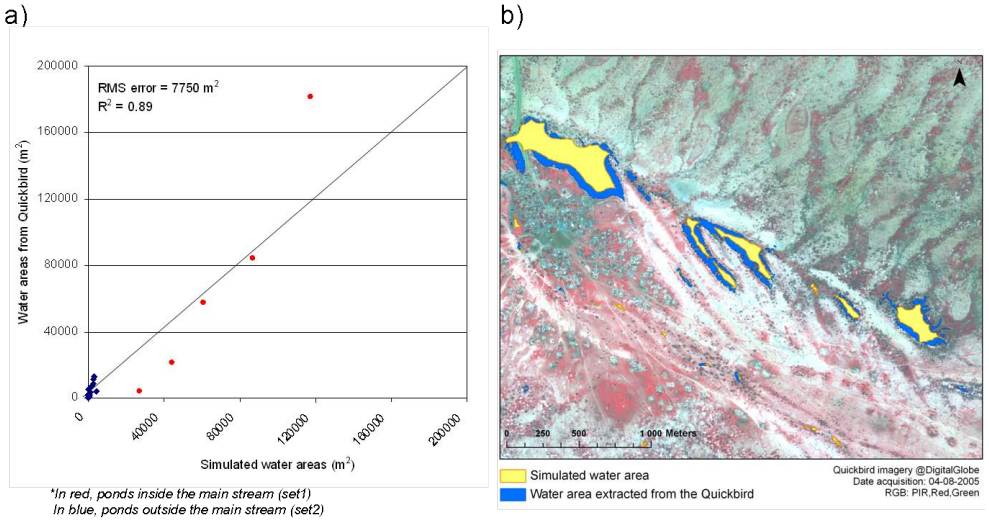

Fig. 7. Comparison of observed (Quickbird imagery, 20 August 2007) and modelled water areas; **(a)** Graphical representation of the observed water area derived from Quickbird imagery versus modelled water areas, and **(b)** Map of the observed (in blue) and modelled (in yellow) water areas, Barkedji, Senegal. To represent simulated pond surface areas on the map, a buffer was applied to the observed pond polygons to trim them to the simulated surface area. The thickness of the buffer to be applied for each pond was determined by calculating the pond radius as $\sqrt{(A/\pi)}$, with A the simulated surface of the pond.

5.4 Model validation

The validation phase showed good agreements between model outputs (water levels and water areas) and observed data. For the years 2001–2002, water height simulations from rain gauge data showed good results for Furdu (Nash=0.87) and Mous 3 (Nash=0.83) which are ponds of similar size, and also for Barkedji (Nash=0.82) the largest pond. For Mous 2 which is much smaller (500 m^2), the result is less significant but still acceptable with a Nash coefficient of 0.70. The simulations using TRMM rainfall data are acceptable for the rainy season 2002 for Furdu pond (Nash=0.73), Barkedji (Nash=0.66) but very poor for the rainy season 2001. This difference may be due to an important underestimation of the rainfall TRMM satellite, especially for the year 2001 (−100 mm recorded by TRMM compared with the gauge) and missed rain events due to rainfall spatial heterogeneity that characterize the Sahel region (Ali et al., 2005). At the rain-event scale, over an area corresponding to a square degree, D'Amato and Lebel (1998) have estimated that on average, 26% of the surface area do not receive rain. The rain events missed by the satellite have an important impact on water height estimations and particularly during the filling phase (see Fig. 6) which determine the maximum volume of the pond for one rainy season. As shown in the sensitivity analysis, the model is sensitive to k and G_{max} which are used in the calculation of inflow runoff. This could explain that less rain or missed events could have important consequence on the water height simulations.

When comparing with pond water area extracted form the 20 August 2007 Quickbird satellite image, model simulations are found to underestimate observed values (Fig. 7a). One explanation could be that, as for the 2001 and 2002 rainy seasons, daily rainfall is underestimated in TRMM data. However, good correlations were obtained for the ponds inside the main stream (set 1) and weak ones for the ponds outside the main stream (set 2), especially those with maximum water areas less than 4000 m^2. That could partly be explained by the uncertainty related to the watershed delineation and to the pond shape parameters. But, regarding the

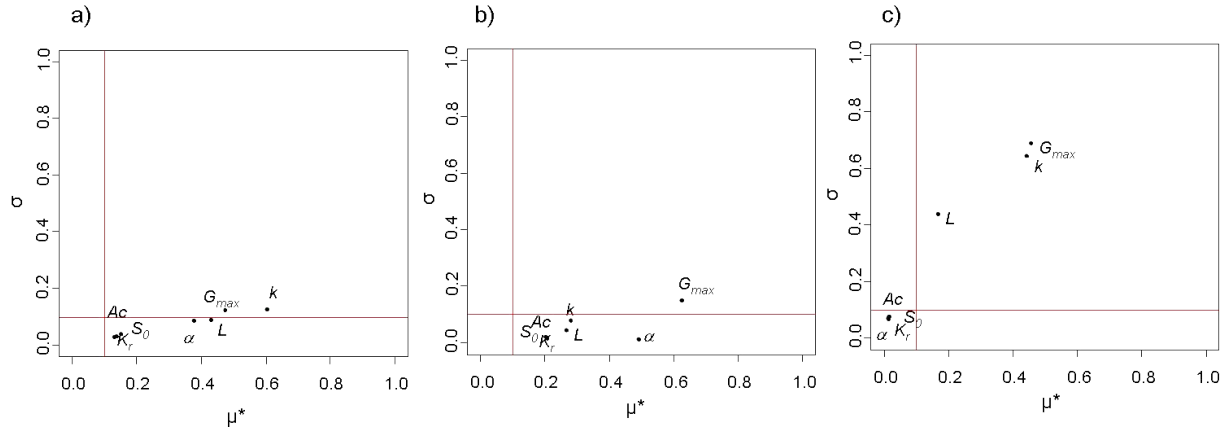

Fig. 8. Results of the Morris OAT sensitivity analysis for three model outputs: **(a)** cumulated water height, **(b)** maximum water height and **(c)** occurrence of the first peak in water height. The graph represents the average of elementary effects in absolute values (μ*) according to their standard deviation (σ) to model outputs. The red lines delimit the space in three types of parameters: i) those with negligible effects (μ*<0.1), ii) those with linear effects on the output, and without interaction between parameters (σ<0.1), iii) those with interactions and/or nonlinear relationship (μ^* >0.1 and σ >0.1).

results of the SA (Fig. 8), the analysis shows that those factors have a small influence on outputs, whereas other factors such as the threshold runoff value have much more influence. The model shows that the smallest ponds are empty while they were not supposed to be, suggesting that the $G_{\max}$ value could be too high for these ponds.

5.5 Model simplifications and possible improvements

Our objective was to develop a simple and robust model in a context of data poor areas; thus, different simplifications have been made. In particular, the pond emptying model is extremely simple as it assumes that the water level decreases constantly with time. If additional data were available our model could be refined to take into account temporal changes in evapotranspiration which is affected by air temperature, humidity and wind speed. Another improvement could be to take into account the infiltration decrease in the clogged area (Porphyre et al., 2005). Nevertheless, this would imply estimating the height of this area for each pond, depending on soil properties. In our study, we assumed that the rainfall was uniformly distributed over the study area; this assumption is obviously not justified, but, again, this simplification is compatible with the simplicity of the model and the available data. Rainfall measurements from only one rain gauge were used. All the ponds were within 8 km from the rain gauge location. But ponds for which water level measurements were made, and on which validations were carried out, were within 3 km. By using a dense network of rain gauges near Niamey (Niger), Taupin (1997) showed that rainfall variability in the Sahel could in fact be high even at a sub-kilometre scale. This simplification may explain some of the discrepancies between observed and simulated water heights.

5.6 The use of remote sensing data

In our study area, the use of very high spatial resolution imagery (Quickbird) was required to locate and estimate pond surface area, including the smallest ponds $<1100\,m^2$ (Soti et al., 2009). But because of a common compromise between spatial and temporal resolution of Earth Observation Systems, such sensors may only provide few images a year and are inappropriate for a daily follow-up of water areas. Our results however showed that coupling hydrologic modelling with remote sensing is relevant when assessing the spatio-temporal dynamics of water bodies in the Sahelian region. The SA showed that the catchment area parameter did not have a large effect on model simulations. Nevertheless, the use of ASTER data (pixel size 30 m×30 m) for catchment area estimation of the larger ponds significantly improved the simulations in comparison with those obtained previously (not shown) with the Shuttle Radar Topographic Mission (SRTM) DEM (pixel size 90 m×90 m). For such areas characterized by low elevation, it was almost impossible to extract pond catchment area with the SRTM DEM.

The model was first run using gauge rainfall measurements as input, but because of the difficulty to have gauge measurements wherever necessary, we tested rainfall estimated from satellite as model input. Given the spatial heterogeneity of the rain events (Balme et al., 2005, 2006) that characterizes the study area, an under- or overestimation of TRMM rainfall (Fig. 6) against the rain gauge is not surprising because TRMM data averages rain events occurring in a 0.25°×0.25° grid. Climate model are far from resolving the small scale variability of rainfall (Balme et al., 2006) and results of the simulation with 2001 rain TRMM data showed that rain estimates by TRMM satellite are yet too inaccurate to be directly used to force fine scale hydrological models (Vischel

et al., 2009). Our simulations showed mixed and irregular results especially for water heights with clearly better results for year 2002.

5.7 Application of the model

This pond modelling work was carried out within the context of a wider study on the Rift Valley Fever, a mosquito-borne disease that affects ruminant herds which rely mostly on ponds for water in the semi-arid Sahelian zone of northern Senegal. The dynamics of water height and surface area of the ponds largely determine the dynamics of mosquito abundance around the ponds. Thus, the need to develop a simple model was to be able to simulate pond water dynamics accurately enough (i) to subsequently help understand the dynamics of mosquito abundance, and (ii) to better assess changing water availability for moving herds. With respect to these objectives, the results of the validation phase can be considered promising. The outputs of the model (changes in water surface area during the rainy season) can be fed into a population dynamics model and be applied on all the ponds of the study area. Although TRMM data tend to underestimate rainfall, the timing is usually correct. For this reason, it is expected that model simulation of mosquito abundance would not suffer a lot from this underestimation problem. These first results may also be useful for other disciplines with specific questions in relation to the assessment of water resource dynamics. In ecology, for instance, it may be interesting to use the model to better understand fauna spatial distribution and mobility in areas with temporary ponds (Redfern et al., 2003) or to support water resources management.

Overall, our results show that it is possible to apply the model to all the ponds of the Ferlo Valley, of which the study area is representative. Moreover, the methodology developed is simple, and could be implemented in other areas. This would require the following data i) water heights and rainfall field data collected daily at least during two rainy seasons ii) one high spatial resolution satellite image acquired at the peak of the rainy season to locate and estimate the maximum area of the water bodies iii) a DEM to estimate the catchment areas. Pond shape parameters S_0 and α require detailed ground survey for their estimation, and may therefore be more difficult to obtain. However, the simple geometric relationship has been in use for a long time, and S_0 and α values for very different water bodies exist in the literature (e.g. Piaton and Puech, 1992; Nilsson et al., 2008). The present study suggests that pond shape parameters estimated for a given pond could also be used for other similar ponds.

6 Conclusions

In this paper, a simple hydrologic pond model was developed and applied to all ponds of the study area located in the Ferlo Valley, North Senegal. Remote sensing data were used to estimate some of the model parameters: a Quickbird image was used to locate and estimate the maximum surface area of water bodies and the ASTER DEM was used to delineate the watershed of the larger ponds. Rainfall estimated from satellite (TRMM data) as model input was also tested in comparison with gauge rainfall measurements. Results showed the possibility of successfully assessing the spatial and temporal dynamics of pond water levels and water areas in a homogeneous area with a simple hydrologic model coupled with satellite imagery. Our method is particularly suited to the context of remote and data poor areas.

Acknowledgements. This research was funded by the EDEN (Emerging diseases in a changing European environment – http://www.eden-fp6project.net/) project. It is officially catalogued by the EDEN Steering Committee as EDEN0124. The contents of this publication are the sole responsibility of the authors and do not necessarily reflect the views of the European commission. Water height, rainfall and bathymetric survey data were obtained from Centre de coopération Internationale en Recherche Agronomique pour le Développement (CIRAD), Institut Sénégalais de la Recherche Agricole (ISRA) and Institut de Recherche pour le Développement (IRD) supported by the EMERCASE Project ("ACI Télémédecine" grant), funded by the French Ministry of Research. The pond map derived from the Quickbird imagery acquired the 20 August 2007 were obtained from the IRD supported by the API-AMA Project. The authors wish to thank Christian Baron, Véronique Chevalier, Pascal Degenne, Raphael Duboz, Agnès Bégué (CIRAD), Flavie Cernesson (CEMAGREF) and Guillaume Jubelin (SAS Nevantropic) for their help and fruitful discussions during this study. We also thank G. Di Baldassarre and three anonymous reviewers for their comments and suggestions on the earlier version of the manuscript. They significantly contributed to its amelioration.

Edited by: G. Blöschl

References

Ali, A., Lebel, T., and Amani, A.: Rainfall Estimation in the Sahel. Part I: Error Function, J. Appl. Meteorol., 44, 1691–1706, 2005.

Anctil, F., Michel, C., Perrin, C., and Andréassian, V.: A soil moisture index as an auxiliary ANN input for stream flow forecasting, J. Hydrol., 286, 155–167, 2004.

Annor, F. O., van de Giesen, N., Liebe, J., van de Zaag, P., Tilmant, A., and Odai, S. N.: Delineation of small reservoirs using radar imagery in a semi-arid environment: A case study in the upper east region of Ghana, Phys. Chem. Earth, 34, 309–315, 2009.

Balme, M., Galle, S., and Lebel, T.: Analysis of the variability of the onset of the rainy season in the Sahel at hydrological and agronomical scales, based on EPSAT-Niger data, Secheresse, 16, 15–22, 2005.

Balme, M., Vischel, T., Lebel, T., Peugeot, C., and Galle, S.: Assessing the water balance in the Sahel: Impact of small scale rainfall variability on runoff: Part 1: Rainfall variability analysis, J. Hydrol., 331, 336–348, 2006.

Barton, I. J. and Bathols, J. M.: Monitoring floods with AVHRR, Remote Sens. Environ., 30, 89–94, 1989.

Bengtsson, L. and Malm, J.: Using rainfall-runoff modeling to interpret lake level data, J. Paleolimnol., 18, 235–248, 1997.

Campolongo, F. and Braddock, R., The use of graph theory in the sensitivity analysis of the model output: a second order screening method, Reliability Engineering and System Safety, 1–12, 1999.

D'At de Saint Foulc, J., Gilard, O., and Piaton, H.: Petits barrages en terre au Burkina Faso. Bilan et analyse critique, CIEH, Ouagadougou, 180, 1986.

D'Amato, N. and Lebel, T.: On the characteristics of rainfall events in the Sahel, with a view to the analysis of climatic variability, Int. J. Climatol., 18, 955–974, 1998.

Desconnets, J. C.: Typologie et caractérisation hydrologique des systèmes endoréiques en milieu sahélien (Niger, degré carré de Niamey), University of Montpellier, 326 pp., 1994.

Desconnets, J. C., Taupin, J. D., and Leduc, C.: Hydrology of the HAPEX-Sahel Central Super-Site: surface water drainage and aquifer recharge through the pool systems, J. Hydrol., 188–189, 155–178, 1997.

Di Baldassarre, G., Schumann, G., and Bates, P. D.: A technique for the calibration of hydraulic models using uncertain satellite observations of flood extent, J. Hydrol., 367, 276–282, doi:10.1016/j.jhydrol.2009.01.020, 2009.

Dingzhi, P., Lihua, X., Shenglian, G., and Ning, S.: Study of Dongting Lake area variation and its influence on water level using MODIS data, Hydrol. Sci. J., 50, 31–44, 2005.

Diop, A. T., Diaw, O. T., Diémé, I., Touré, I., Sy, O., and Diémé, G.: Ponds of the Sylvopastoral Zone of Senegal, Revue Élev. Méd. Vét. Pays trop., 57, 77–85, 2004.

Dubreuil, P. L.: Review of Relationships between Geophysical Factors and Hydrological Characteristics in the Tropics, J. Hydrol., 87, 201–222, 1986.

FAO: Crue et apports. Manuel pour l'estimation décennal et des apports annuels pour les petits bassins versants non jaugés de l'Afrique sahélienne et tropicale sèche, Bulletin FAO d'irrigation et de drainage, Rome, 1996.

Frappart, F., Hiernaux, P., Guichard, F., Mougin, E., Kergoat, L., Arjounin, M., Lavenu, F., Koité, M., Paturel, J.-E., and Lebel, T.: Rainfall regime across the Sahel band in the Gourma region, Mali, J. Hydrol., 375, 128–142, 2009.

Gates, D. J. and Diessendorf, M.: On the fluctuations in levels of closed lakes, J. Hydrol., 33, 267–285, 1977.

Girard, G.: Les modèles hydrologiques pour l'évaluation de la lame d'eau écoulée en zone sahélienne et leurs contraires, Cahier de l'Orstom, Paris, 189–221, 1975.

Haas, E., Combal, B., and Bartholomé, E.: A map of temporary water bodies in Western Africa. GlobWetland: Looking at Wetlands from Space, ESA Publications Division, Frascati, Italy, 2006.

Hayashi, M. and Van der Kamp, G.: Simple equations to represent the volume–area–depth relations of shallow wetlands in small topographic depressions, J. Hydrol., 237, 74–85, 2000.

Heggen, R. J.: Normalized antecedent precipitation index, J. Hydrol. Eng., 6, 377–381, 2001.

Herold, N. D., Haack, B. N., and Solomon, E.: An evaluation of radar texture for land use/cover extraction in varied landscapes, Int. J. Appl. Earth Obs., 5, 113–128, 2004.

Horritt, M. S., Mason, D. C., and Luckman, A. J.: Flood boundary delineation from synthetic aperture radar imagery using a statistical active contour model, Int. J. Remote Sens., 22, 2489–2507, 2001.

Joannes, H., Parnot, J., Rantrua, F., and Sow, N.: Possibilité d'utiliser la télédetection dan sle domaine de l'eau en Afrique, CIEH Série hydrologie, 141, 1986.

Kohler, M. A. and Linsley, R. K.: Predicting runoff from storm rainfall, US Weather Bureau Research Paper, 34, 1951.

Lacaux, J. P., Tourre, Y. M., Vignolles, C., Ndione, J. A., and Lafaye, M.: Classification of ponds from high-spatial resolution remote sensing: Application to Rift Valley Fever epidemics in Senegal, Remote Sens. Environ., 106, 66–74, 2007.

Lange, J., Leibundgut, C., Greenbaum, N., and Schick, A. P.: A noncalibrated rainfall–runoff model for large, arid catchments, Water Resour. Res., 35, 2161–2172, 1999.

Le Houerou, H. N.: Introduction au Projet Ecosystèmes pastoraux sahéliens, FAO, Rome, 42, 1988.

Lebel, T., Diedhiou, A., and Laurent, H.: Seasonal cycle and interannual variability of the Sahelian rainfall at hydrological scales, J. Geophys. Res., 108, 8389, doi:10.1029/2001JD001580, 2003.

Liebe, J., van de Giesen, N., and Andreini, M.: Estimation of small reservoir storage capacities in a semi-arid environment, Phys. Chem. Earth, 30, 448–454, 2005.

Linthicum, K. J., Kaburia, H. F., Davies, F. G., and Lindqvist, K. J.: A blood meal analysis of engorged mosquitoes found in Rift Valley fever epizootics area in Kenya, J Am Mosq Control Assoc, 1, 93–95, 1985.

Martin-Rosales, W. and Leduc, C.: Variability of the dynamics of temporary pools in a semiarid endoreic system (southwestern Niger), Hydrology of Mediterranean and Semiarid Regions, 174–178, 2003.

McFeeters, S. K.: The use of the normalised difference water index (NDWI) in the delineation of open water features, Int. J. Remote Sens., 17, 1425–1432, 1996.

Montanari, M., Hostache, R., Matgen, P., Schumann, G., Pfister, L., and Hoffmann, L.: Calibration and sequential updating of a coupled hydrologic-hydraulic model using remote sensing-derived water stages, Hydrol. Earth Syst. Sci., 13, 367–380, doi:10.5194/hess-13-367-2009, 2009.

Morris, M.: Factorial sampling plans for preliminary computational experiments, Technometrics, 33, 161–174, 1991.

Nash, J. E. and Sutcliffe, J. V.: River flow forecasting through conceptual models. Part I: A discussion of principles, J. Hydrol., 10, 282–290, 1970.

Ndiaye, P. I.: Modélisation de la dynamique de population des moustiques Aedes en zoe sahélienne. ewemple des Aedes vexans arabiensis (Diptera: cilicidae) vecterus de la fièvre de la vallée du Rift en Afrique de l'ouest, PHD, Metz University and Gaston Berger de Saint Louis University, 125 pp., 2006.

Nilsson, K. A., Ross, M. A., and Trout, K. E.: Analytic method to derive wetland stage-storage relationships using GIS areas, J. Hydrol. Eng., 13, 278–282, 2008.

O'Connor, D. J.: Seasonal and long-term variations of dissolved solids in lakes and reservoirs, J. Environ. Eng., 115, 1213–1234, 1989.

Piaton, H. and Puech, C.: Apport de la télédétection pour

l'évaluation des ressources en eau d'irrigation pour la mise en valeur des plans d'eau à caractère permanent ou semi-permanent au Niger. Rapport de synthèse, Comité Interafricain d'Etudes Hydrauliques, 150, 1992.

Pin-Diop, R., Touré, I., Lancelot, R., Ndiaye, M., and Chavernac, D.: Remote sensing and géographic information systems to predict the density of ruminants, hosts of Rift Valley fever virus in the Sahel, Vet. Ital. Ser., 42, 675–686, 2007.

Porphyre, T., Bicout, D. J., and Sabatier, P.: Modelling the abundance of mosquito vectors versus flooding dynamics, Ecol. Model., 183, 173–181, doi:10.1016/j.ecolmodel.2004.06.044 2005.

Puech, C.: Plans d'eau sahéliens et imagerie SPOT: inventaire et évaluation des capacités d'exploitation, Colloque international "Eau, environnement et développement", Nouakchott, Mauritanie, 68–83, 1994

Puech, C. and Ousmane, A.: Gestion régionale de plans d'eau sahéliens par télédétection : courbes de fonctionnement, suivi annuel et reconstitution de chroniques hydrologiques, Eau et développement durable : témoignages de la société civile, Paris, 42–44, 1998

Redfern, J. V., Grant, R., Biggs, H., and Getz, W. M.: Surface-water constraints on herbivore foraging in the Kruger National Park, Ecology, 84, 2092–2107, 2003.

Saltelli, A., Tarantola, S., Campolongo, F., and Ratto, M., Sensitivity Analysis in Practice: A Guide to Assessing Scientific Models, John Wiley & Sons publishers, 232, 2004.

Sandholt, I., Nyborg, L., Fog, B., Lô, M., Bocoum, O., and Rasmussen, K.: Remote sensing techniques for flood monitoring in the Senegal River Valley, Geogr. Tidsskr., 103, 71–81, 2003.

Schumann, G., Bates, P. D., Horritt, M. S., Matgen, P., and Pappenberger, F.: Progress in Integration of Remote Sensing-Derived Flood Extent and Stage Data and Hydraulic Models, Rev. Geophys., 47, RG4001, doi:10.1029/2008RG000274, 2009.

Soti, V., Chevalier, V., Maura, J., Tran, A., Etter, E., Lelong, C., Sow, D., Ndiaye, M., Sall, B., Thiongane, Y., Lancelot, R., and De Laroque, S.: Landscape characterization of Rift Valley Fever risk areas using very high spatial resolution imagery: case study in the Ferlo area, Senegal, GIS Vet, Copenhagen, Denmark, 2007

Soti, V., Tran, A., Bailly, J.-S., Puech, C., Lo Seen, D., and Bégué, A.: Assessing optical Earth Observation Systems for mapping and monitoring temporary ponds in arid areas, Int. J. Appl. Earth Obs., 11, 344–351, doi:10.1016/j.jag.2009.05.005, 2009.

Taupin, J.-D.: Caractérisation de la variabilité spatiale des pluies aux échelles inférieures au kilomètre en région semi-aride (région de Niamey, Niger), Comptes Rendus de l'Académie des Sciences – Series IIA - Earth and Planetary Science, 325, 251–256, 1997.

Tourre, Y. M., Lacaux, J. P., Vignolles, C., Ndione, J. A., and Lafaye, M.: Mapping of zones potentially occupied by Aedes vexans and Culex poicilipes mosquitoes, the main vectors of Rift Valley fever in Senegal, Geospatial Health, 3, 69–79, 2008.

Verdin, J. P.: Remote sensing of ephemeral water bodies in Western Niger, Int. J. Remote Sens., 17, 733–748, 1996.

Vischel, T. and Lebel, T.: Assessing the water balance in the Sahel: Impact of small scale rainfall variability on runoff. Part 2: Idealized modeling of runoff sensitivity, J. Hydrol., 333, 340–355, 2007.

Vischel, T., Lebel, T., Massuel, S., and Cappelaere, B.: Conditional simulation schemes of rain fields and their application to rainfall-runoff modeling studies in the Sahel, J. Hydrol., 375, 273–286, 2009.

Wheater, H., Sorooshian, S., and Sharma, K. D., Hydrological Modelling in Arid and Semi-Arid Areas, University Press, Cambridge, 195, 2007.

Wilson, M. L., Chapman, L. E., Hall, D. B., Dykstra, E. A., Ba, K., Zeller, H. G., Traorelamizana, M., Hervy, J. P., Linthicum, K. J., and Peters, C. J.: Rift-Valley Fever in Rural Northern Senegal - Human Risk-Factors and Potential Vectors, Am. J. Trop. Med. Hyg., 50, 663–675, 1994.